arXiv:0812.2847v1 [astro-ph] 15 Dec 2008

The Frequency of Warm Debris Disks and Transition Disks in a Complete Sample of Intermediate-Mass GLIMPSE Stars: Placing Constraints on Disk Lifetimes

B. Uzpen [1], H. A. Kobulnicky [1],

and

K. Kinemuchi [2 3]

ABSTRACT

The incidence of dusty debris disks around low- and intermediate-mass stars has been investigated numerous times in order to understand the early stages of planet formation. Most notably, the *IRAS* mission observed the entire sky at mid- and far-IR wavelengths, identifying the first debris disk systems, but was unable to detect a statistically significant sample of warm debris disks due to its limited sensitivity at 12 μm. Using Tycho-2 Spectral Catalog stars previously shown to exhibit 8 μm mid-infrared circumstellar excesses confirmed at 24 μm in the *Spitzer* GLIMPSE survey, we investigate the frequency of mid-IR excesses among intermediate-mass (2–4 $M_{\odot}$) stars in a complete volume-limited sample. Our study of 338 stars is four times larger than a complete sample of 12 μm sources from the *IRAS* Point Source Catalog. We find that 0.3±0.3% of intermediate-mass stars exhibit a signature of a possible terrestrial-temperature debris disks at wavelengths of 8 μm and greater. We also find that 1.2±0.6% of intermediate-mass stars exhibit evidence for circumstellar disks undergoing inner disk clearing, i.e., candidate transition disk systems. Using stellar lifetimes and the frequency of transition and primordial disks within a given spectral type, we find that pre-main-sequence disks around intermediate-mass stars dissipate in 5±2 Myr, consistent with other studies.

Subject headings: methods: statistical — stars: statistics, stars: circumstellar matter

[1]University of Wyoming, Dept. of Physics & Astronomy, Dept. 3905, Laramie, WY 82071

[2]Departamento de Astronomía, Universidad de Concepción, Casilla 160-C, Concepción, Chile

[3] Department of Astronomy, University of Florida, 211 Byrant Space Science Center, Gainesville, Florida 32611-2055, USA

1. Introduction

While it is generally accepted that most stars are surrounded by primordial gaseous circumstellar accretion disks when they are formed (e.g., Waters & Waelkens 1998), and that they gradually disperse, some evolving toward dust-only "debris disks" containing processed grains (Backman & Paresce 1993), there are gaps in understanding how these two types of disks are connected. From color-color studies of the "Big Four" debris disks (Vega, Fomalhaut, ϵ Eridani, and β Pictoris) it has been noted that debris disks may form a continuum from very dusty systems, such as β Pictoris, to less dusty systems such as Vega (Backman et al. 1987; Decin et al. 2003). By studying the evolution of circumstellar disks and determining the relative frequency of each evolutionary stage, one may place constraints on the timescales of planet formation. In this paper we conduct such a study of late-stage disks around a large sample of intermediate-mass (2–4 $M_{\odot}$) stars—a population lacking, until recently, sufficient representation in infrared surveys to draw statistical conclusions.

Studies of individual star forming regions and stellar clusters have concluded that primordial disks around intermediate-mass stars dissipate more rapidly than their low-mass counterparts (e.g., Dahm & Hillenbrand 2007). The timescales for this dissipation vary from less than 3 Myr (Hernández et al. 2005) up to ∼5 Myr (Carpenter et al. 2006), while low-mass objects may take as long as 10 Myr (Sicilia-Aguilar et al. 2006). However, most cluster studies contain only a few to a few tens of intermediate-mass stars, rendering the estimates for disk clearing timescales in this mass range uncertain. The time it takes for circumstellar disks to dissipate is critically related to planet formation. The two most prominent planet formation theories propose drastically different time scales for the formation of planets, with core-accretion (Goldreich & Ward 1973; Mizuno 1980) requiring up to 8 Myr (Mordasini et al. 2007) and gravitational disk instability (Kuiper 1951) requiring less than 0.1 Myr (Boss 1997). Constraining the time necessary for disk clearing can test the validity of planet formation theories. Disk dissipation timescales of much less than 3 Myr would imply rapid planetary formation and lend support to the disk instability theory or require a refinement of the core-accretion theory.

Toward the end of the primordial disk phase, the gaseous circumstellar disk begins to dissipate, and with it, the signature of the infrared excess. Primordial disks are characterized by large circumstellar excesses at wavelengths greater than 1 μm indicated by their fractional infrared luminosities (L_{IR}/L_{*}) greater than 10^{-2} (Hillenbrand et al. 1992). Later-stage disks, however, have smaller fractional infrared luminosities and do not exhibit near-IR excesses ($<$ 5 μm), which indicates that the inner portion of the disk is largely devoid of material. Such late-stage disks with mid-IR (5–12 μm) excesses and inner holes, but containing primordial material at more distant radii, have been termed "transition disks" (Strom et al. 1989;

Strom & Najita 2005). Transition disks were once thought to be rare, and their rarity implied rapid circumstellar disk dissipation (e.g., Wolk & Walter 1996). A majority of known transition disks surround low-mass ($\sim$1 $M_{\odot}$ FGK-type) stars (Najita et al. 2007), for example, TW Hya (Calvet et al. 2002). Recently, many new low-mass transition disks have been identified, and they may comprise $\sim$10% of the pre-main-sequence population (Cieza et al. 2007). By comparison, only a few candidate transition disks have been identified around intermediate-mass stars (Hernández et al. 2006; Hernandez et al. 2007; Uzpen et al. 2008). The lack of a large sample of transition disks around intermediate-mass stars may imply different circumstellar evolutionary paths for different mass stars, or may reflect the difficulty in observing transition disks in a statistically meaningful sample of intermediate-mass stars.

Debris disks are the final chapter in the circumstellar evolutionary sequence. As a second generation disk of processed dust generated by grain growth and planetesimal collisions, debris disks have fractional infrared luminosities less than 10^{-2}, with most exhibiting fractional infrared luminosities less than 10^{-4} (Artymowicz 1996). Debris disks were first identified by the *Infrared Astronomical Satellite* (*IRAS*) on the basis of an excess emission at $\lambda > 25$ μm detected during routine calibrations of Vega (Aumann et al. 1984). Subsequently, many debris disks have been identified through the comparison of optical catalogs with the *IRAS* catalog (e.g., Rhee et al. 2007). At least 15% of nearby A–K main-sequence stars have dusty debris disks that were detectable with *IRAS* and *Infrared Space Observatory* (*ISO*) sensitivities in the far-infrared (Meyer et al. 2006; Lagrange et al. 2000; Backman & Paresce 1993). Plets & Vynckier (1999) found the disk fraction (the fraction of systems exhibiting disks) for main-sequence stars and their descendants to be 13$\pm$10% and 14$\pm$5%, respectively, at 60 μm. Investigating 160 A-type stars, Su et al. (2006) found that 32$\pm$5% of their sample exhibits an excess at 24 μm. More recently, Hillenbrand et al. (2008) determined that $\sim$10% of 0.6–1.8 $M_{\odot}$ main-sequence stars exhibit 70 μm emission characteristic of debris disks. Debris disks may be indicators of planetary systems (Zuckerman & Song 2004), and Beichman et al. (2005) found that 24$\pm$10% of the stars exhibiting emission at 70 μm due to dust also have planetary systems, while Moro-Martín et al. (2007) found that $\sim$10% of FGK stars have planets regardless of disk presence. Debris disks identified to have planets are both cool (T $<$ 200 K) and 10–100 times more massive than the debris within our solar system (Beichman et al. 2005). No planet has yet been identified in a debris disk system exhibiting shorter wavelength infrared excesses ($<$ 12 μm) due, in part, to the scarcity of such sources.

Studies using *IRAS* and the *ISO* have shown a systematic drop in infrared excess with stellar age for debris disks (Spangler et al. 2001; Habing et al. 2001). Observing 266 A-type stars with the *Spitzer Space Telescope* (*Spitzer*), Rieke et al. (2005) found that excess emission decreases with age as t_0/t with t_0=150 Myr. Su et al. (2006) found a similar trend

between fractional infrared luminosity and stellar age along with evidence that the inner portions of debris disks clear more rapidly than the outer portions. Bryden et al. (2006) investigated 69 FGK main-sequence stars and found that 2±2% of stars exhibited $L_{IR}/L_* > 10^{-4}$ with one star of the sample showing evidence of warm dust (T > 200 K). Moór et al. (2006) investigated 60 debris disks within 120 pc and found that nearly all the stars with $(L_{IR}/L_*) > 10^{-4}$ are young with ages less than 100 Myr. These results are consistent with previous studies that conclude disk clearing occurs on short time-scales, at young ages, and form from the inside out (e.g., Habing et al. 2001; Decin et al. 2003; Mamajek et al. 2004 and references therein).

Mid-IR excess debris disk sources, such as β Pictoris, appear to be extremely rare (Chen et al. 2005). Stars that exhibit a mid-infrared excess have characteristic disk temperatures of 200–1000 K. Dust with these temperatures surrounding intermediate-mass stars is located between ∼1–25 AU, and such regions are analogous to our asteroid belt. By comparison, long-wavelength excesses (> 24 μm) have cooler (T∼100 K) dust located farther from the central star and are more comparable to the Kuiper Belt. Aumann & Probst (1991) investigated 548 nearby main-sequence stars using 12 μm measurements from *IRAS* and found that only 2 stars (< 0.5%) exhibited genuine excesses confirmed from ground based observations. Aumann & Probst (1991) also found that out of the 35 nearby A-type stars, only β Pictoris exhibited a strong 10 μm excess, resulting in a disk fraction of less than 3%. Prior to *Spitzer*, only three intermediate-mass main-sequence or near-main-sequence stars exhibited a strong mid-IR excess: β Pictoris, ζ Leporis, and HR 4796A (Aumann & Probst 1991; Metchev et al. 2004). Eta Cha and HD 3003 exhibit a weak 12 μm excess in the *IRAS* Faint Source catalog (Mannings & Barlow 1998) and Vega exhibits a weak near-IR excess (Absil et al. 2006). Prior to *Spitzer*, only three intermediate-mass stars were known to be surrounded by disks predominately composed of warm dust with disk temperatures greater than 200 K: η Cha, ζ Leporis, and HD 3003 (Mannings & Barlow 1998; Chen & Jura 2001; Rhee et al. 2007). With the vastly superior sensitivity of *Spitzer*, a number of *IRAS* 60 μm excess debris disks have been shown to have excesses at shorter wavelengths (8.5–13 μm; Chen et al. 2006). *Spitzer* has also been used to identify a number of new candidate warm (T > 200 K) debris disk systems around early type stars that exhibit excesses at 8 and 24 μm (Uzpen et al. 2005; Uzpen et al. 2007; Hernández et al. 2006; Currie 2008).

In this paper, we present the statistical detection rates for a complete[1] survey of intermediate-mass (2–4 $M_\odot$) mid-IR excesses of indeterminate age identified in the *Spitzer* Galactic Legacy Infrared MidPlane Survey Extraordinaire (GLIMPSE; Benjamin et al. 2003).

[1]We use the word "complete" to mean volume-limited sample constructed by applying a Malmquist bias correction to a flux-limited sample.

The goal of this paper is to compare the disk fractions of warm debris disks and transition disks in a sample of field stars to a compilation of young cluster members and to determine the timescales for pre-main-sequence disk dissipation around intermediate-mass stars. Some of these field stars may be young stars of yet unidentified clusters since warm debris disks are most common around stars of age 10–15 Myr (Currie et al. 2008). In §2, we discuss how we obtained our sample of warm debris and transition disks drawn from optical, spectral, and infrared catalogs following the results of Uzpen et al. (2007, 2008). In §3 we determine our statistically complete working sample. We also examine the constraints our survey places on planetary formation and circumstellar disk evolution. In §4, we compare the constraints our sample places on the longevity and frequency of transition disk systems and the frequency of warm debris disks to other studies. We conclude, in §5, that debris disks and transition disk systems are rare and may help constrain circumstellar disk evolution scenarios.

2. The Warm Debris Disk/Transition Disk Sample

Our stellar sample draws upon the Tycho-2 Spectral Catalog (Wright et al. 2003), 2MASS all-sky survey (Cutri et al. 2003), and GLIMPSE Catalog (v1.0). The Tycho-2 Spectral Catalog contains more than 351,000 positional matches of stars with known spectral types from major spectral catalogs, such as the Henry Draper Catalog, with the Tycho-2 Catalog (Høg et al. 2000) that contains both B and V photometric data and high quality astrometric data. The GLIMPSE project is one of six original *Spitzer* Legacy Programs. GLIMPSE mapped the Galactic Plane at 3.6, 4.5, 5.8, and 8.0 μm with sensitivities of 0.6, 0.6, 2, and 10 mJy, respectively. The GLIMPSE Catalog identified over 3×10^7 sources within the survey region. In the GLIMPSE data reduction pipeline, JHK photometry was obtained from 2MASS images, and the 2MASS sources were cross-correlated with GLIMPSE sources. Our resultant complete working sample has both spectral information and photometric measurements in the B, V, J, H, K, [3.6], [4.5], [5.8], and [8.0] bandpasses.

In Uzpen et al. (2007), we identify 22 intermediate-mass stars in the Tycho-2 Catalog and GLIMPSE survey of luminosity class V or IV and spectral type B8 or later that exhibit 8 μm mid-infrared extraphotospheric excesses. These excess sources were identified from among more than 4,000 stars investigated. The sample contained 1,024 stars with luminosity class V or IV of which 493 were of spectral type B8–A5. Six of the 22 stars with infrared excesses did not have luminosity classifications in the Tycho-2 Spectral Catalog. Instead, the luminosity classifications were derived from observations in Uzpen et al. (2007) and classified therein. These six stars were removed from the statistical analysis of our complete working sample, in §3 and 4, because they lacked a luminosity classification within the Tycho-2

Spectral Catalog. We confirmed the excess at 8 μm by finding an excess at 24 μm for 11 of the 16 remaining stars in Uzpen et al. (2007, 2008). Ten of the 11 remaining stars were observed as part of the sample in Uzpen et al. (2008) to determine the origin of their infrared excess. Four of the 10 stars exhibited Hα emission and were found to have an excess owing to free-free emission. Four of the stars exhibited Hα emission at a level insufficient to explain their infrared excess owing to free-free emission. The excesses for these four sources were consistent with blackbody emission from warm dust, and these sources were classified as candidate transition disks. One star exhibited Hα emission and optical spectral features characteristic of Herbig AeBe (HAeBe) stars and is a candidate class II protostar. One of the 10 sources, G311.0099+00.4156, did not exhibit Hα emission and is a candidate warm debris disk. Table 1 lists the six stars exhibiting excesses ascribed to warm dust. This table also shows stellar parameters (effective temperature, rotational velocity, Hα equivalent width) and circumstellar parameters (disk temperature and fractional infrared luminosity) from Uzpen et al. (2008). The K-[8.0] and [8.0]-[24.0] colors are taken from Uzpen et al. (2007). Other terms have been used to define disks undergoing disk clearing, e.g., "anemic disks" (Lada et al. 2006). We use the term "transition disk" to mean a dissipating disk with evidence of circumstellar gas, a fractional infrared luminosity between 10^{-2}–10^{-4}, and an infrared excess due to dust. As reported in Uzpen et al. (2008), transition disk systems do not exhibit Paschen emission lines, may exhibit O I λ8446 emission, or O I λ7772 in emission or absorption, do not exhibit Fe II emission, and must have an excess at 8 and 24 μm not entirely explainable by free-free emission. Presumably, transition disks contain some primordial gaseous material as evidenced by their gaseous emission lines. For the purposes of this paper, transition disks are part of the group of disks, including class II protostellar disk systems, that comprise primordial (pre-main-sequence) disk systems. Therefore, both transition and class II protostellar disk systems will be used to determine timescales for primordial disk clearing. Warm debris disks are stellar systems lacking gaseous emission with dust temperature of 200–1000 K that exhibit infrared circumstellar excesses at 5–12 μm and longer wavelengths. To summarize, our sample of 493 B8–A5 luminosity class IV-V stars from GLIMPSE, 2MASS, and Tycho-2 Spectral Catalogs contains four transition disks, one class II protostellar disk object, and one warm debris disk.

3. Approach to Constructing a Volume-Limited Sample

Like any flux-limited survey, use of the GLIMPSE catalog is subject to Malmquist bias (Malmquist 1922). Generically, this effect arises from an inherent dispersion of absolute magnitude, σ_M, among a sample of similar stars such that more luminous objects scatter into a flux-limited sample because they are detected at greater distances (Binney & Merrifield

1998; Gilmore et al. 1990). For our study, this potentially results in stars with 8 μm excesses preferentially being detected to larger distances than non-excess stars, thereby biasing the disk fractions toward higher values. In general terms, the *measured mean absolute magnitude*, $\bar{M}_{mag}$, that would be observed in a flux-limited sample is brighter than the *true mean absolute magnitude*, $\bar{M}_{vol}$, by a small factor that depends upon σ_M and $A(m)$, which is the star count function $dN(m)/dm$. Mathematically, Gilmore et al. (1990) show that

$$\bar{M}_{mag} = \bar{M}_{vol} - ln10 \times \sigma_M^2 \frac{dlogA(m)}{dm}. \quad (1)$$

Similarly, in the absence of interstellar extinction, the *measured mean apparent magnitude*, $\bar{m}_{mag}$, that would be observed in a flux-limited sample is brighter than the *true apparent magnitude*, $\bar{m}_{vol}$, in a volume-limited sample,

$$\bar{m}_{mag} = \bar{m}_{vol} - ln10 \times \sigma_M^2 \frac{dlogA(m)}{dm}. \quad (2)$$

Defining a volume-limited sample for a group of similar spectral type stars requires knowledge of $\bar{m}_{vol}$ (effectively the apparent magnitude limit of the survey) which we will call m_{lim} and $\bar{M}_{vol}$ (usually based upon stellar models or calibrated standard spectral types). The limiting radial distance is then determined from the usual distance modulus,

$$r = 10^{0.2\times(\bar{m}_{mag}-\bar{M}_{vol})+1}. \quad (3)$$

Interstellar extinction at the wavelength of interest, A_λ, constitutes an additional factor that will act to drive the completeness limit toward *fainter* apparent magnitudes. A survey is volume-limited (i.e., complete) at magnitudes brighter than $m_{comp} \equiv \bar{m}_{mag} + A_\lambda$. Selecting all stars with $m < m_{comp}$ yields a volume-limited sample within radial distance r.

3.1. Construction of the Complete Working Sample

Both $\bar{M}_{vol}$ and σ_M can be measured from a sample of stars with well-determined distances, and we use the *Hipparcos* (Perryman et al. 1997) parallaxes in the All-sky Compiled Catalogue of 2.5 million stars (Kharchenko 2001) to estimate these values. As a test of our analysis methods, we computed $\bar{M}_{vol}$ and σ_M for a sample of 352 K0V stars and compared our results to those of Butkevich et al. (2005) and Oudmaijer et al. (1999) who analyzed similar stars using the same *Hipparcos* dataset. We rejected the most uncertain measurements by requiring that the parallaxes be positive and have $S/N \equiv \pi/\sigma_\pi > 3$, leaving 347 stars. We

used the listed Tycho-2 spectral types and observed $B-V$ colors to reddening correct each star assuming a standard interstellar extinction law and R=3.1. The top portion of Figure 1 shows the distribution of absolute magnitudes for the 347 remaining K0V stars. The histogram has a narrow, roughly Gaussian core with broad, asymmetric wings, most notably on the bright side. This asymmetry may be understood as the result of unresolved binaries and misclassified giants. In an effort to cleanse the sample of these possible contaminants, we remove stars more than 3σ from the mean using a sigma clipping algorithm. The resultant sample contains 208 stars and is shown by the dash-dot-dot histogram. The dashed line in the top plot of Figure 1 is a Gaussian distribution with mean of $\bar{M}_{vol}$=5.62±0.14 mag and a dispersion of $\sigma_M = 0.29$ mag that characterizes the remaining 208 stars. By comparison, Butkevich et al. (2005) found $\bar{M}_{vol} = 5.81 \pm 0.01$ and $\sigma_M = 0.33 \pm 0.02$ for a sample of 45 K0V stars fainter than 4.5 mag carefully chosen to remove binaries and possible spectral misclassifications. Oudmaijer et al. (1999) found $\bar{M}_{vol} = 5.69$ and $\sigma_M = 0.40$ for a sample of 85 K0V stars with distances less than 50 pc and V magnitudes greater than 4.5. In summary, we determine estimates for $\bar{M}_{vol}$ and σ_M that are consistent with those in the literature, suggesting that the same approach will yield suitable values for applying a Malmquist bias corrections to our B8V – A5V sample. However, all three studies of K0V stars result in slightly brighter measured mean absolute V magnitudes than the 5.9 mag tabulated in Cox (2000). These studies used by Cox (2000), (i.e., Aller et al. 1982; Johnson 1966; de Jager & Nieuwenhuijzen 1987), are prior to the launch of *Hipparcos*. Distances calculated from *Hipparcos* were improved, which may explain the slight discrepancies. Regardless, the small differences between the *Hipparcos* determined $\bar{M}_{vol}$ values (< 0.2 mag) have a small effect ($< 10\%$) on the definition of our volume-limited sample and subsequent conclusions.

Our similar analysis of 1,095 A0V stars with *Hipparcos* parallactic measurements yields $\bar{M}_{vol} = 0.92 \pm 0.20$ and $\sigma_M = 0.65$. The lower plot in Figure 1 shows the distribution of the full sample and a Gaussian distribution having the same mean and dispersion as the 772 stars that remain after outlier rejection. We find that the dispersion of absolute magnitudes is approximately twice as large for early-type stars compared to late-type stars. This implies that there is either an intrinsically greater dispersion of luminosity in early-type stars or there is a greater uncertainty in the classification of early-type stars. Additional reddening uncertainties may affect the intermediate-mass sample to a greater extent than the lower-mass sample, leading to a larger dispersion. The median distance for the K0V sample is 50 pc, while the A0V sample median distance is 220 pc. Small deviations of our assumed reddening law results in dispersions four times greater for early-type stars compared to late-type stars. Our adopted value of $\sigma_M = 0.65$ may, therefore, be regarded as a conservative upper limit that, when used to correct for Malmquist bias, yields a relatively small volume-

limited sample of intermediate-mass stars.

The parameter $A(m)$ describes the differential star count per apparent magnitude bin, which in turn depends upon the space density distribution and the stellar luminosity function. Under the simplifying assumption of a homogeneously distributed population having a Gaussian luminosity function, Binney & Merrifield (1998) show that the factor (d log A(m)/dm)=(d ln A(m)/ ln 10)/dm in Equation 2 reduces to 0.6. At the distances probed by our survey (<1 kpc) and at $|b| < 1°$, all of our intermediate-mass stars will have $|z|$ <20 pc, thereby falling within the thin disk of the Milky Way (Haywood et al. 1997) where the assumption of homogeneity is a reasonable one. Equation 2 then reduces to

$$\bar{m}_{mag} = \bar{m}_{vol} - \sigma_M^2 \times 0.6. \tag{4}$$

For A0V stars, the final term in Equation 4 becomes $0.65^2 \times 0.6 = 0.25$, meaning that our sample becomes volume-limited at apparent magnitudes 0.25 mag brighter than the nominal flux limit of the least sensitive dataset required for inclusion in the survey. We require inclusion in the Tycho-2 Catalog (99% complete to V=11 (Høg et al. 2000)), the 2MASS Catalog (99% complete to K=14.3 (Cutri et al. 2003)), and the GLIMPSE Catalog (99.5% complete to 10 mJy at IRAC band 4). The GLIMPSE limit is equivalent to [8.0]=9.52 mag. For spectral types near A0 that typify our sample, the completeness limit of the GLIMPSE [8.0] data is ultimately the limiting factor in constructing our "complete working sample", to be defined below.

In order to construct our complete working sample we passed Kurucz ATLAS9 model atmosphere spectra through digitized photometric bandpasses using temperatures and surface gravities corresponding to the nearest spectral type to determine V-[8.0] colors (Kurucz 1993). Since all of the stars lie within the solar circle, we adopt the solar metallicity models. For an A0V star we use the stellar model of temperature 9,500 K with surface gravity of log g=4.0. The resulting colors were then used to determine our limiting magnitude. For example, an A0V star was found to have V-[8.0]=0.06. In the absence of reddening we found that an A0V star with M_V=0.92 determined from the parallaxes above will reach the [8.0] limit at 540 pc with $V \equiv m_{lim}$=9.58. Similarly, an A5V star will reach the [8.0] limit at 520 pc with $V \equiv m_{lim}$=9.89 and a B8V star will reach the [8.0] limit at 730 pc with $V \equiv m_{lim}$=9.28.

As an average value for interstellar extinction, we adopt $A_V = 1.5$ mag kpc^{-1}. Our assumed value of extinction does not affect our distance limit. Only the computed V band limits are affected by extinction, with greater extinction pushing our V band limits to fainter values. Since A_V is $\lesssim$1.0 mag for distances up to $\sim$ 700 pc in our survey, it has a small effect on m_{comp}, our completeness limit, which is always brighter than the V-band limits

of the Tycho-2 catalog. If A_V exceeds 2.5–3 magnitudes then our correction for Malmquist bias would require an iterative process between distance completeness limits and m_{comp} with reddening affecting our distance limit. We solve for m_{comp} using,

$$m_{comp} = \bar{m}_{mag} + 0.015[mag\ pc^{-1}] \times r[pc]. \quad (5)$$

As mentioned above, an A0V star reaches the 10 mJy limiting [8.0] flux equivalent of $V \equiv m_{lim} = 9.58$ at a distance of 540 pc in the absence of extinction and Malmquist bias corrections. However, $9.58 - 0.65^2 \times 0.6$ implies $\bar{m}_{mag}$=9.33, corresponding to a volume-limited distance of 480 pc. After applying a correction for extinction, we find that A0V stars at a distance of 480 pc have $m_{comp} = 10.05$. Table 2 lists the distances, D_{sp}, and m_{comp}, at which each spectral subtype, B8V through A5V, is volume-limited. These distances and magnitudes define our "complete working sample".

In addition to our flux limit of 10 mJy at [8.0], our sample has a brightness limit at [8.0] of 700 mJy, which is the saturation limit for IRAC and corresponds to a $V \simeq 5$ star. There are only two luminosity class V stars brighter than V=5 in the complete GLIMPSE working sample. Both of these stars are of spectral type A5, and have [5.8] and [8.0] measurements in GLIMPSE although they have quality flags, and they are saturated in the [3.6] and [4.5] bandpasses. Since we could determine whether these stars exhibit an excess at [8.0], we included them in our sample. For an unreddened B8V star, this saturation limit occurs at $V \sim 4.7$ mag and 87 pc and for an A5V star, the saturation limit occurs at $V \sim 5.3$ mag and 58 pc.

3.2. Detection and Constraints on Disk Longevity from the Complete Working Sample

Using the method outlined above, we find that there are 338 stars between B8–A5 and luminosity class V and IV in the volume where our sample is complete for each respective spectral type within the Tycho-2 and the GLIMPSE surveys. Table 3 shows the number of stars of luminosity class V (column 2) or IV (column 3) within the complete GLIMPSE working sample at each spectral type. Stars listed as IV in our sample are either luminosity class IV or IV/V stars and do not include III/IV stars from the Tycho-2 Spectral Catalog. Table 3 shows that our sample is mostly comprised of B9 and A0 stars (175) with just a small fraction later than A2 (36).

Column 9 of Table 1 shows that our one warm debris disk candidate (G311.0099+00.4156), our one class II protostellar disk (G321.7868+00.4102), and all four transition disk can-

didates (G305.4232–00.8229, G307.9784–00.7148, G311.6185+00.2469, G314.3136–00.6977) fall within the magnitude limits of the complete GLIMPSE working sample. The implied detection rates are then 0.3±0.3% ($1/338\pm\sqrt{1}/338$) for warm debris disks and 1.2±0.6% (4/338) for transition disk candidates, and 1.5±0.7% for all pre-main-sequence disks (class II protostellar and transition disks) surrounding intermediate-mass stars. The lifetime of a B8 star (4 $M_{\odot}$) is 150 Myr, whereas a B9 star (3.5 $M_{\odot}$) is 220 Myr and an A1 star (2.7 $M_{\odot}$) is 430 Myr (Siess et al. 2000). The fraction of systems with transition disks times the stellar lifetime yields an empirical statistical estimate for the duration of the transition disk phase. Transition disks are the end points of pre-main-sequence circumstellar disks, and including them with the number of class II protostellar disks times the stellar lifetime provides insight into the time necessary for pre-main-sequence disks to dissipate.

We found 45 B8 stars within the complete working sample. Two of these 45 stars exhibited transition disk features for a detection rate of 4.4±3.1%. Given that the lifetime of a B8 star is 150 Myr, our detection rate implies a lifetime of 6±4 Myr (4.4±3.1%×150 Myr) for transition disks or 4.4% the lifetime of a B8 star. We identified one transition disk, out of 93 B9 stars within our sample, and that led to a detection rate of 1.1±1.1%. The implied lifetime of a B9 tranistion disk is then 2±2 Myr. There are 56 A1 stars within the sample, and we found only one transition disk yielding a detection rate of 1.8±1.8%. Using the lifetime of 430 Myr for an A1 star, we find that transition disks persist for 8±8 Myr. The results for B8, B9, and A1 stars are consistent with one another but do not provide strong constraints on the transition disk duration.

Considering the whole sample, we have a detection rate of four out of 338 sources for transition disks and are able to place a greater constraint on the transition disk lifetime. This is done for a range of spectral types rather than one spectral sub-class. Most of our stars are of spectral types A0 and B9. In order to better estimate the longevity of transition disks, we approximate the mean lifetime of our sample. Table 5 shows the number of stars for a given spectral type and the calculated lifetime for that star based on Siess et al. (2000) evolutionary models of the nearest stellar mass to the measured spectral type. We determine that the weighted mean lifetime of our sample is 360 Myr using the lifetime and the number of stars at a given spectral type within our sample. Given our detection rate, we estimate the lifetime of transition disk systems to be 4±2 Myr (i.e., 4/338 × 360 Myr). In Uzpen et al. (2008) we estimate the age of G307.9784–00.7148, a transition disk system, to be 1–2 Myr, consistent with the lifetime for these types of objects. Unfortunately, these results do not provide strong enough evidence to show that disks do indeed undergo rapid inner disk clearing on timescales less than 1 Myr (Wood et al. 2002), nor do these results lend support to either of the two leading planet formation theories. These results do, however, demonstrate that terrestrial-temperature material around intermediate-mass stars is quite rare. Systems that

exhibit terrestrial-temperature dust are ideal candidates for follow-up observations to identify Earth-like planets.

If we include transition disks in our sample of pre-main-sequence disks, we can make an estimate of the lifetime of primordial circumstellar disks around intermediate-mass stars. Looking at our sample as a whole, we identified five pre-main-sequence disks (4 transition and 1 class II) out of 338 sources. Using a weighted mean lifetime of 360 Myr, we determine that primordial disks persist for 5±2 Myr. This result is consistent with cluster studies where disk clearing occurs within ∼6 Myr (Haisch et al. 2001). We summarize our results in Table 4 for the disk fraction of warm debris, transition, and class II protostellar disks within the sample population and the primordial disk dissipation timescale for each restriction considered.

3.3. The $V \leq 9.25$ Sample

While the Tycho-2 catalog is 99% complete to $V = 11.0$, the Tycho-2 Spectral catalog from which our sample is selected, contains spectral type and luminosity class information for only a subset of these stars. The brightest stars have essentially complete spectral classification, while classifications for stars fainter than $V \sim 9$ become increasingly incomplete, and this potentially introduces a bias in the sample. Figure 2 is a histogram of Tycho apparent magnitude, m_{V_T}, for the Tycho-2 Catalog, which contains 2.5 million stars and the Tycho-2 Spectral Catalog containing 351,000 stars. Although, the Tycho-2 Catalog is complete to $V = 11.0$, the two histograms start to diverge in the 9.25–9.5 histogram bin. Taking the ratio of star counts per bin in the Tycho-2 Spectral Catalog to the Tycho-2 Catalog, we find that this ratio is 88% for the 9.25–9.50 magnitude bin. This means that for stars in Tycho-2 Spectral Catalog at magnitudes fainter than 9.25, we do not expect all the stars to have spectral types yet determined. Our results may be biased into the sense that we require a star to have a spectral classification. For example, if the fraction of disk-bearing pre-main-sequence stars increases toward fainter magnitudes, our results may be biased.

We investigate whether requiring a spectral type affects our results by defining a revised sample with spectral information restricted to objects brighter than $V = 9.25$, the "$V \leq 9.25$ sample". This restricted sample is listed in Table 6. This revised sample contains 163 of the original 338 stars. The warm debris and class II protostellar disks are still detected in this smaller cropped sample. Thus, the resulting disk fraction for warm debris disks is 0.6±0.6%. We now detect one A1 transition disk out of 19 stars, yielding a fraction of 5.3±5.3% and an age upper limit of 23±23 Myr. The one B9 transition disk falls outside the 9.25 magnitude sample limit. The detection rate for B8 stars is two out of 19 stars yielding a disk fraction of 11±7% and an age upper limit of 16±11 Myr. For this entire sample, the

fraction of transition disks is three out of 163 sources, or 1.8±1.1%, yielding an age range of 6±4 Myr. The disk fraction for pre-main-sequence objects is four out of 163 sources, 2.5±1.2%, resulting in an upper limit for disk clearing of 9±4 Myr. The revised magnitude constraint yields a larger lifetime for transition disk systems and also a larger uncertainty compared to our complete working sample. However, the results are still consistent with our values from the complete working sample, suggesting that the incompleteness of the Tycho-2 Spectral Catalog does not introduce large biases. Working under the presumption that the spectral types identified consist of a representative sample of intermediate-mass stars at our magnitude limit, we use our complete working sample.

3.4. The Malmquist Biased Sample

Prior to correcting for Malmquist bias, our sample consisted of 493 stars of spectral types B8–A5 and luminosity class IV or V and we will refer to this sample as the "biased sample." Within this sample there were four transition disk systems, one warm debris disk system, and one class II protostellar disk system leading to detection rates of 0.8±0.4% for transition disks, 0.2±0.2% for warm debris disks, and a primordial disk detection rate of 1.0±0.5%. All three of these biased detection rates are consistent with the complete working sample results. Using our weighted mean stellar lifetime of 360 Myr, the biased detection frequency of transition disks implies that this phase persists for 3±1 Myr. This result also implies primordial disks clear within 4±2 Myr and is consistent with stellar cluster studies (e.g., Lada et al. 2006) that find most primordial circumstellar disks clear within 5 Myr.

3.5. Additional Analysis and Consistency Check

Taken at face value, our findings indicate that transition disks can persist longer than the ∼1 Myr predicted from observations and seem to be more common than the lack of detections in previous observational studies would suggest (Skrutskie et al. 1990; Wolk & Walter (1996); Wood et al. 2002; Cieza et al. 2007). Using our selection criteria, transition disks are more common than their progenitors, HAeBe stars, contrary to expectations. However, this may simply be the result of small number statistics. We considered whether some selection effect would preferentially exclude HAeBe stars from our sample. While there is no explicit criterion excluding these objects, their copious circumstellar material produces systematically higher visual extinctions. For example, the well-studied HAeBe stars from Hillenbrand et al. (1992) have extinctions and distances that imply $A_V \gg 1.5$ mag kpc^{-1}, suggesting that in many such objects, circumstellar extinction dominates over interstellar

extinction. Such a circumstellar component would cause HAeBe stars to drop out of the Tycho-2 Spectral Catalog from which our complete sample is drawn and thereby explain their deficit in our statistics.

As an independent means of estimating the relative frequencies of HAeBe stars, transition disk systems, and their main-sequence descendants, we used 2MASS near-IR and GLIMPSE mid-IR colors to identify objects of each evolutionary stage within the GLIMPSE survey area. The top plot of Figure 3 shows a J–H vs. H–K diagram. This color space is commonly used to distinguish pre-main-sequence stars (HAeBe stars) from their main-sequence counterparts (Hernández et al. 2005). We take the unreddened color box of Hernández et al. (2005) Figure 2 and apply A_V=10 to the upper bounds of that box in order to define a region where we would expect to find reddened HAeBe stars. Nearly all of the HAeBe stars from Hillenbrand et al. (1992) fall within this box. Therefore, we assume that this region will include most HAeBe stars. Most lower-mass pre-main-sequence stars (T-Tauri) from Hartmann et al. (2005) fall outside the HAeBe region and are not a major source of contamination. Our transition disk candidates, by definition lacking near-IR excesses, and β Pictoris, a well-known debris disk system, fall outside the HAeBe region and lie near the main-sequence. We define a hexagonal region in this figure to estimate where most B and A main-sequence stars can be found. The boundaries of the hexagon are chosen to encompass unreddened B8–A5 main-sequence stars and reddened B8 stars with $A_V \leq 4$. Extending the hexagon further to the upper right (toward larger extinction) would begin to include substantial numbers of reddened low-mass main-sequence stars and possible T-Tauri stars. The bottom plot of Figure 3 shows a *Spitzer* IRAC [4.5]–[8.0] vs. J–K color-color diagram. This color space is useful for distinguishing transition disk candidates from other types of stars. The symbols are the same as those in the upper plot of Figure 3. The rectangular region defines objects with [8.0] excesses where we find most transition disks. We know from Uzpen et al. (2008) that this region is contaminated by some mid-IR excess debris disks and classical Be stars. However, this region provides the least contaminated space for identifying transition disk candidates, and we will correct our estimate for this contamination.

Using the defined color regions we identify ∼5,600 candidate HAeBe stars, ∼3,300 transition disk candidates, and ∼194,000 potential B- and A-type main-sequence stars. Using the fraction of classical Be stars found in the transition disk color space (∼1/3) from Uzpen et al. (2008), we estimate that at most 2,200 of these stars would be true transition disk objects. The transition disk fraction of 2,200/194,000 or 1% is consistent with our prior results. The fraction of pre-main-sequence objects, i.e., HAeBe and transition disk objects, is ((5,600+2,200)/194,000)=4%. This fraction is higher than our value of 1.5±0.7% within our complete working sample. However, our value is roughly consistent with the above analysis

given that the populations are likely to have some contamination and given the differing levels of extinction used to define the samples. Using these raw numbers we find that the transition disk lifetime may be as long as one-third (2,200/(5,600+2,200)) the primordial disk lifetime. Using our estimate of 4±2 Myr for the transition disk lifetime, this result would imply that the primordial disk lifetime is 12±6 Myr. Although long, this value is consistent, within uncertainties, with disk clearing studies. Conversely, if we were to use our estimated primordial disk lifetime of 5±2 Myr, we find that transition disks survive 2±1 Myr. Our result of 2±1 Myr is longer than that estimated by Cieza et al. (2007). Our result is consistent with other studies, which find transition disk objects occur within 1–10 Myr (e.g., Cieza et al. 2007), but is longer than their estimated timescale for disk clearing of 0.4 Myr. In summary, the possible omission of HAeBe stars from our complete working sample is not likely to be a large effect, given that we arrive at similar results for the transition disk lifetime and primordial disk lifetime from an independent, albeit more uncertain, approach.

4. Comparison to Other Studies

In order to place our results in context of circumstellar disk evolution scenarios, we compare the derived fractions to those of other infrared surveys for circumstellar disks using *IRAS* and *Spitzer*. This comparison allows us to determine if improved infrared sensitivity and the larger volume surveyed by GLIMPSE places greater constraints on mid-IR excess frequency. We also compare our results to a compilation of all equivalent mass stars in *Spitzer*-studied young star clusters (< 10 Myr). Young star clusters contain both primordial circumstellar disks and second generation dust disks. By comparing equivalent-mass stars over a small age range, 1–10 Myr, we can determine if the warm debris disk fraction and disk dissipation times are consistent.

4.1. *IRAS*

IRAS was flux-limited at 0.5 Jy in the 12 μm band. This limit for an A5V star occurs at V=5.0. Applying Malmquist bias corrections we find that the *IRAS* survey was complete to a distance of 44 pc for intermediate-mass stars. There are 84 stars in the Tycho-2 Spectral Catalog that fall within a complete flux-limited *IRAS* sample of B8–A5 spectral types with IV or V luminosity class. We use this band to compare the warm debris disk fraction to the *IRAS* Catalog. One of the 84 *IRAS* stars, β Pictoris, has a 12 μm excess indicative of a mid-IR excess debris disk or about 1.2±1.2%. Zeta Leporis, the other known *IRAS* 12 μm excess, does not appear in the Tycho-2 Spectral Catalog and is omitted from this

analysis. The GLIMPSE survey is complete at distances of 58–410 pc for intermediate-mass stars. GLIMPSE surveyed 220 deg^2 of the celestial sphere or 220/41253 of the solid angle *IRAS* covered. Therefore, the GLIMPSE survey is complete to an equivalent sphere of 72 pc in radius. This constitutes ∼4 times the volume of the *IRAS* survey. Our result for the frequency of mid-IR debris disks, $0.3 \pm 0.3\%$, is consistent with the value from the *IRAS* survey, while encompassing four times the volume, leading to smaller uncertainties.

Transition disks were not detected with *IRAS* but are present in ∼1% of our sample. The reason for this discrepancy may be due to the relative volumes covered. *IRAS* was an all-sky survey, while GLIMPSE focused more on the Galactic Plane. The GLIMPSE survey was designed to observe the majority of high-mass Galactic star forming regions and has identified a number of new Galactic clusters (Mercer et al. 2005; Kobulnicky et al. 2005; Strader & Kobulnicky 2008). *IRAS* did not go deep enough to be complete at the nearest star forming regions. Since the disk fraction is correlated with age (e.g., Rieke et al. 2005), one would preferentially see more excesses in the younger Galactic Plane population of the GLIMPSE survey. This could result in the increased detection rate of transition disks in our working sample.

4.2. Spitzer Studies of Young Star Clusters

One of the major goals of *Spitzer* was to increase our understanding of stellar and circumstellar evolution in the context of planet formation. To achieve that goal, a number of General Observer, Guaranteed Time Observer, and Legacy programs have observed stellar clusters and star forming regions over a large range of ages. In order to understand the process of circumstellar disk dissipation, at least 16 stellar clusters have been observed by *Spitzer* over the 1–11 Myr age range (summarized in Hernandez et al. 2008). We culled from the literature 165 B8–A5 stars for the following clusters and associations: σ Ori (8; Hernandez et al. 2007), γ Velorum (14; Hernandez et al. 2008), NGC 2362 (2; Dahm & Hillenbrand 2007), η Cha (1; Megeath et al. 2005), NGC 7160 and Tr 37 (18 and 10; Sicilia-Aguilar et al. 2006), Orion OBIa and OBIb (14 and 18; Hernández et al. 2006), IC 348 (7; Lada et al. 2006), Upper Sco (35; Carpenter et al. 2006), NGC 1333 (3; Gutermuth et al. 2008), and NGC 2244 (35; Balog et al. 2007). These clusters have *Spitzer* IRAC and/or MIPS data with spectral types in either the associated paper or other related papers found using SIMBAD. Twelve of these stars are surrounded by primordial circumstellar disks. Figure 4 shows the primordial disk fraction versus age (Myr) for these 12 clusters. This figure shows that the incidence of primordial disks is zero at ages greater than 4 Myr, indicating that primordial disks around intermediate-mass stars dissipate within the first 4–5 Myr. By comparison, Hernandez et al.

(2008) Figure 11 shows that disk dissipation around low-mass stars is a slower process, requiring 10–15 Myr. This result is consistent with individual cluster studies that find differing disk fractions for intermediate- and low-mass members (e.g., Carpenter et al. 2006). We find disk dissipation occurring within 4±2 Myr based on pre-main-sequence disk fractions within a complete sample of intermediate-mass field stars is in agreement with the disk dissipation rate found within cluster studies.

Using *Spitzer* studies of young star clusters, Currie et al. (2008) found that debris disk fractions increase at ages from 5–10 Myr and peak in the 10–15 Myr range. We found 27 stars identified as debris disk systems out of the 165 B8–A5 cluster stars in recent surveys, yielding a debris disk fraction of 16±3%, which is consistent with other studies of debris disk fraction using data at $\lambda > 24$ μm (e.g., 33±19% at ages < 10 Myr; Rieke et al. 2005). However, only two of the 27 debris disk candidates exhibit warm circumstellar excesses at [8.0], HD 36444 (Hernández et al. 2006) and BD+31 641B (Currie 2008). The frequency of warm debris disks within young stellar clusters, 1.2±0.9%, is consistent with our somewhat more restrictive result of 0.3±0.3% from field stars. This result implies that wide-area surveys containing millions of stars such as GLIMPSE, GLIMPSE II, and GLIMPSE 3D may be ideal laboratories to identify more of these objects, and with more of these unique objects, better studies can be conducted to illuminate the astrophysics of this short stellar evolutionary period.

5. Conclusion

We determined that the incidence of B8–A5 main-sequence stars with warm debris disks is 0.3±0.3%, and transition disks is 1.2±0.6% within a complete sample of the GLIMPSE, 2MASS, and Tycho-2 Spectral Catalogs. The excess fraction measured here is much lower than the 10–20% of main-sequence stars that exhibit far-IR excesses at $\lambda \geq 60$ μm (e.g., Hillenbrand et al. 2008). These mid-IR excess sources may be members of yet-identified young stellar clusters. The rarity of main-sequence stars that exhibit mid-, but not near-IR excesses suggests that this stage of star formation is short-lived, consistent with prior observational results (Wolk & Walter 1996; Cieza et al. 2007).

We find the fraction of transition disk systems in our complete working sample and a more inclusive biased sample are in agreement with one another. Investigation of likely transition and primordial disks, using stellar models and statistical techniques, allows us to constrain the lifetime of B8–A5 primordial circumstellar disks to 5±2 Myr using our complete working sample and 4±2 Myr using a more inclusive sample that is not corrected for Malmquist bias. These values are consistent with those found by a growing number of

studies targeting young stellar clusters using *Spitzer*. Our study provides a complementary measurement using a significantly larger and independently selected sample of intermediate-mass field stars. Further investigation of these sources will help identify the place of mid-IR excess circumstellar disks in the evolutionary process of star and planet formation. However, our results do not provide strong support for either current competing planet formation theories.

The authors would like to thank the anonymous referee for suggestions that improved this paper. We kindly thank M.R. Meade, B.L. Babler, R. Indebetouw, B. A. Whitney, C. Watson, and E. Churchwell for their use of the GLIMPSE data reduction pipeline. We thank Dana Backman and Lynne Hillenbrand for their helpful comments. B.U. acknowledges support from a NASA Graduate Student Researchers Program fellowship, grant NNX06AI28H. This research has made use of the SIMBAD database, operated at CDS, Strasbourg, France. This publication makes use of data products from the Two Micron All Sky Survey, which is a joint project of the University of Massachusetts and the Infrared Processing and Analysis Center/California Institute of Technology, funded by the National Aeronautics and Space Administration and the National Science Foundation.

Table 1. Stellar and Circumstellar Parameters of Disk Systems

ID	K-[8.0] [mag]	[8.0]-[24] [mag]	T_{Disk} (K)	$\frac{L_{IR}}{L_*}$	EW(Hα)$_{corr}$ (Å)	T_{eff} (K)	$v \sin i$ (km s^{-1})	V [mag]	Sp. Type	Comment
(1)	(2)	(3)	(4)	(5)	(6)	(7)	(8)	(9)	(10)	(11)
G305.4232–00.8229	0.79	1.27	675^{+37}_{-33}	$0.0038^{+0.0003}_{-0.0002}$	-21.98±0.42	13520±510	230±20	9.23	B6/8 V(E)	T
G307.9784–00.7148	0.40	1.06	557^{+22}_{-16}	$0.00090^{+0.00007}_{-0.00008}$	-13.27±0.69	13220±520	240±20	7.92	B8 V(N)	T
G311.0099+00.4156	0.37	2.79	315^{+4}_{-3}	$0.0027^{+0.0001}_{-0.0003}$	5.21±0.03	9800±130	235±25	8.07	A3 IV	D
G311.6185+00.2469	0.28	1.82	306^{+13}_{-6}	$0.0012^{0.0001}_{-0.0001}$	-10.90±0.23	10540±255	265±20	9.84	B8/9 IV/V	T
G314.3136–00.6977	0.22	1.45	328^{+11}_{-9}	$0.00096^{+0.00007}_{-0.00008}$	-12.63±0.29	9870±130	205±20	8.49	A1 IV	T
G321.7868+00.4102	0.77	1.25	556^{+18}_{-12}	$0.0021^{+0.0002}_{-0.0001}$	-26.81±0.53	12340±505	230±20	9.16	B8VN	H

Note. — (6) Hα EW corrected for underlying stellar absorption. (11) T: Transition disk, D: Debris disk H: Herbig AeBe disk

Table 2. Survey Completeness Limits

Sp. Type	σ_M[1] [mag]	m_{comp}[2] [mag]	D_{Sp}[3] [pc]
A5V	0.60	10.33	440
A4V	0.79	10.05	410
A3V	0.67	10.15	460
A2V	0.79	9.99	460
A1V	0.65	10.08	470
A0V	0.65	10.05	480
B9V	0.69	9.83	500
B8V	0.69	9.95	640

[1]Measured dispersion in absolute magnitude from *Hipparcos* parallax

[2]Measured m_V at which our sample is complete with assumed reddening

[3]The distance at which our sample is complete.

Table 3. The Complete Working Sample

Sp. Type	N_V[1]	N_{IV}[2]	N_{VIRAS}[3]	N_{IVIRAS}[4]
A5	4	8	5	5
A4	1	3	1	1
A3	11	9	9	4
A2	14	12	5	5
A1	33	23	12	0
A0	63	19	18	7
B9	55	38	6	0
B8	25	20	6	0

[1]Measured number of luminosity class V GLIMPSE sources within the complete sample

[2]Same as (1) for luminosity class IV or IV/V GLIMPSE sources

[3]Measured number of luminosity class V sources within the complete $IRAS$ sample

[4]Same as (3) for luminosity class IV or IV/V $IRAS$ sources

Table 4. Sample Statistics

Sample	DF_{WD} %	DF_T %	DF_P %	$Lifetime_P$ Myr
Complete Working	0.3±0.3	1.2±0.6	1.5±0.7	5±2
$V \leq 9.25$	0.6±0.6	1.8±1.1	2.5±1.2	9±4
Biased	0.2±0.2	0.8±0.4	1.0±0.5	4±2

Note. — See text for sample characteristics and descriptions. DF (Disk Fraction); WD (warm debris disk); T (transition disk); P (Primordial disk)

Table 5. Longevity of Spectral Type

Sp. Type	N_{Stars}[1]	Age[2] Myr
A5	12	980
A4	4	750
A3	20	750
A2	26	530
A1	56	430
A0	82	330
B9	93	220
B8	45	150

[1]Measured number of luminosity class V and IV GLIMPSE sources

[2]Stellar lifetime of Siess et al. (2000) models in Myr for nearest estimated mass to measured spectral type

Table 6. The $V \leq 9.25$ Sample

Sp. Type	N_V[1]	N_{IV}[2]
A5	2	3
A4	1	0
A3	5	3
A2	8	8
A1	15	4
A0	31	10
B9	35	19
B8	14	5

[1]Measured number of luminosity class V GLIMPSE sources within the $V \leq 9.25$ sample

[2]Measured number of luminosity class IV or IV/V GLIMPSE sources within the $V \leq 9.25$ sample

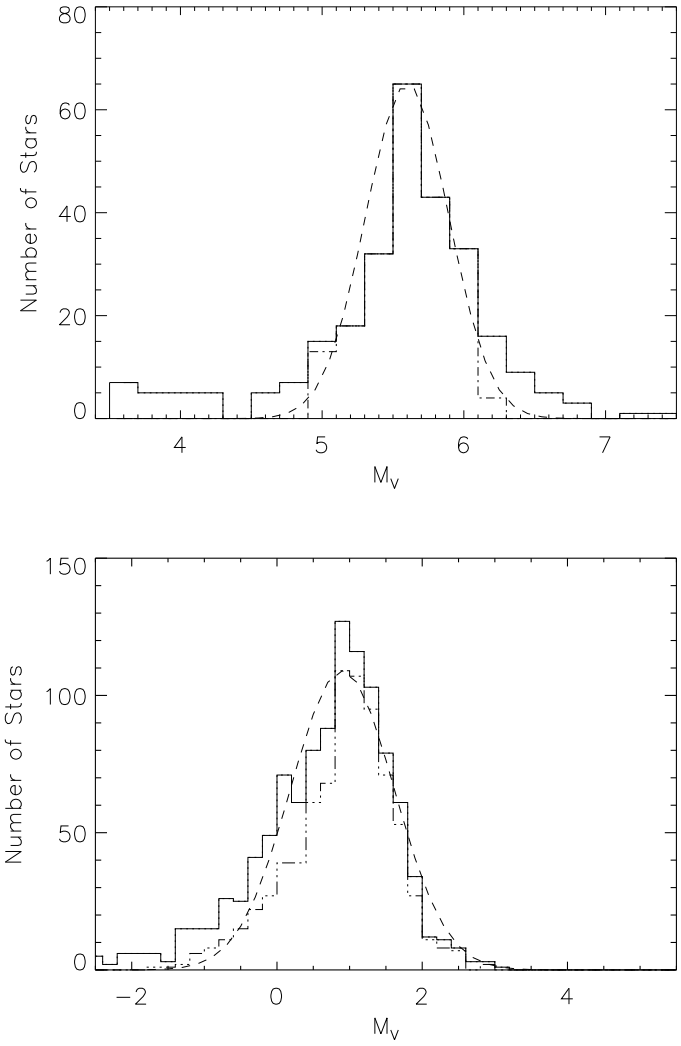


Fig. 1.— (*top*) The distribution of absolute magnitude for 208 K0V stars with *Hipparcos* parallaxes at an S/N > 3. The dashed curve is a Gaussian distribution with a dispersion of 0.29, centered at 5.62, and a maximum equal to the maximum of the K0V histogram. The distribution is nearly Gaussian. (*bottom*) The distribution of absolute magnitude for 772 A0V stars with *Hipparcos* parallaxes at an S/N > 3 in the All-Sky Catalog. The dashed curve is a Gaussian distribution with a dispersion of 0.65, centered at 0.92, and a maximum equal to the maximum of the A0V histogram. The A0V histogram is slightly asymmetric, resulting in a greater dispersion. Similar analyses were performed for all spectral types B8–A5 in order to determine the dispersion in absolute magnitude among each spectral type.

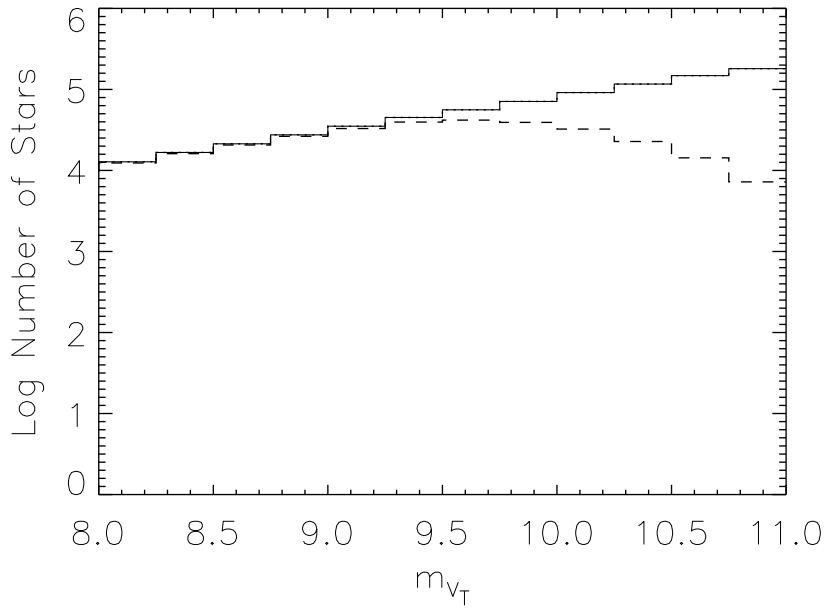


Fig. 2.— Histograms of Tycho visual magnitude for both the Tycho-2 Catalog (*solid line*) and Tycho-2 Spectral Catalog (*dashed line*). The Tycho-2 Spectral Catalog derives its photometric data from the Tycho-2 Catalog and starts to drop off in completeness after 9.25 magnitudes. Therefore, all stars fainter than m_V=9.25 may not have spectral information determined yet.

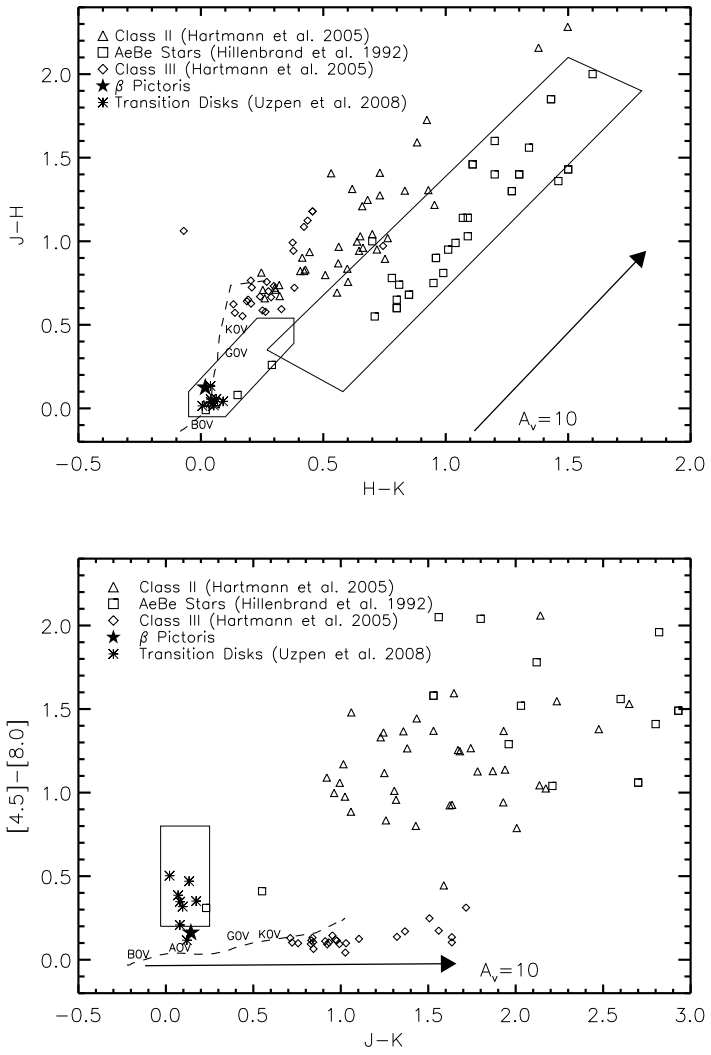


Fig. 3.— (*top*) J–H vs. H–K color diagram. Low-mass pre-main-sequence stars are shown by triangles and diamonds. HAeBe stars are shown by squares and lie in a region that reddened normal main-sequence stars cannot occupy. The fiducial main-sequence is shown by the dashed line. The parallelogram is used to define the region in which we expect to find HAeBe stars. The lower hexagonal region encompasses unreddened B and A main-sequence stars to those with A_V=4. (*bottom*) [4.5]–[8.0] vs. J–K color space. Gaseous pre-main-sequence stars clearly lie above and to the right of the main-sequence. Evolved low-mass pre-main-sequence stars lie to the right of the main-sequence, exhibiting colors consistent with reddening only. Intermediate-mass stars exhibiting excesses consistent with transition disks (*asterisks*) occupy a unique region of color space outlined by the rectangular box. Stars within this box are not highly reddened, exhibit a mid-IR excess, and may be undergoing disk clearing.

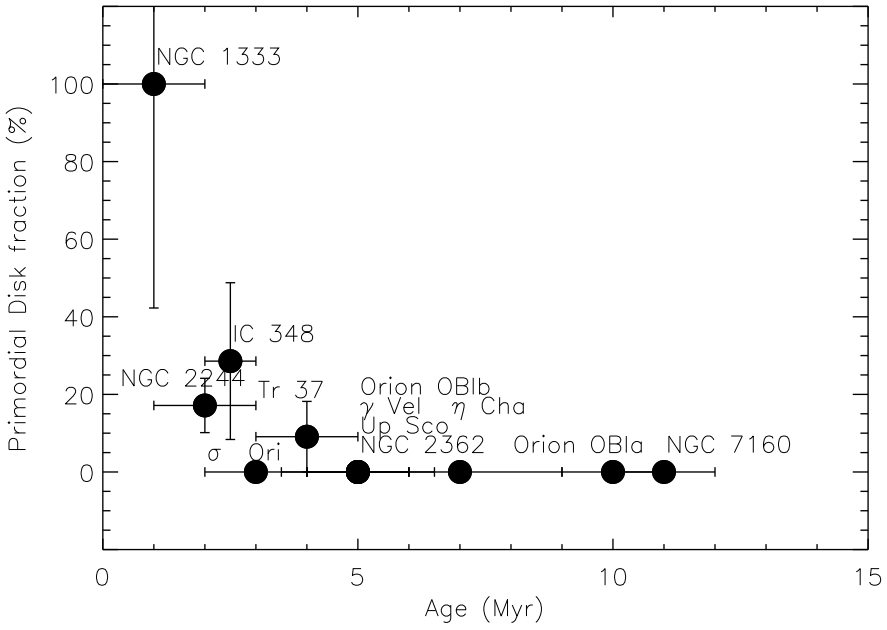


Fig. 4.— Cluster age versus primordial disk fraction for *Spitzer*-observed clusters. None of the clusters older than 4 Myr contain any primordial disks in the spectral range B8–A5. The decay rate is significantly faster than that for cluster members of all masses shown in Hernandez et al. (2008) Figure 11. Orion OBIb, γ Vel, Up Sco, and NGC 2362 are 5 Myr old and contain no primordial disks, therefore their points overlap.

REFERENCES

Absil, O., Di Folco, E., Mérand, A., Augereau, J.-C., Coudé du Foresto, V., Aufdenberg, J. P., Kervella, P., Ridgway, S. T., ten Brummelaar, T. A., & McAlister, H. A. 2006, in Presented at the Society of Photo-Optical Instrumentation Engineers (SPIE) Conference, Vol. 6268, Advances in Stellar Interferometry. Edited by Monnier, John D.; Schöller, Markus; Danchi, William C.. Proceedings of the SPIE, Volume 6268, pp. 626809 (2006).

Aller, L. H., Appenzeller, I., Baschek, B., Duerbeck, H. W., Herczeg, T., Lamla, E., Meyer-Hofmeister, E., Schmidt-Kaler, T., Scholz, M., Seggewiss, W., Seitter, W. C., & Weidemann, V. 1982, Landolt-Börnstein: Numerical Data and Functional Relationships in Science and Technology - New Series " Gruppe/Group 6 Astronomy and Astrophysics " Volume 2 Schaifers/Voigt: Astronomy and Astrophysics / Astronomie und Astrophysik " Stars and Star Clusters / Sterne und Sternhaufen (Landolt-Bornstein: Numerical Data and Functional Relationships in Science and Technology)

Artymowicz, P. 1996, in The Role of Dust in the Formation of Stars, ed. H. U. Käufl & R. Siebenmorgen, 137–+

Aumann, H. H., Beichman, C. A., Gillett, F. C., de Jong, T., Houck, J. R., Low, F. J., Neugebauer, G., Walker, R. G., & Wesselius, P. R. 1984, ApJ, 278, L23

Aumann, H. H., & Probst, R. G. 1991, ApJ, 368, 264

Backman, D. E., Gillett, F. C., Low, F. J., Neugebauer, G., Witteborn, F. C., & Aumann, H. H. 1987, in Bulletin of the American Astronomical Society, Vol. 19, Bulletin of the American Astronomical Society, 830

Backman, D. E., & Paresce, F. 1993, in Protostars and Planets III, ed. E. H. Levy & J. I. Lunine, 1253–1304

Balog, Z., Muzerolle, J., Rieke, G. H., Su, K. Y. L., Young, E. T., & Megeath, S. T. 2007, ApJ, 660, 1532

Beichman, C. A., Bryden, G., Rieke, G. H., Stansberry, J. A., Trilling, D. E., Stapelfeldt, K. R., Werner, M. W., Engelbracht, C. W., Blaylock, M., Gordon, K. D., Chen, C. H., Su, K. Y. L., & Hines, D. C. 2005, ApJ, 622, 1160

Benjamin, R. A., Churchwell, E., Babler, B. L., Bania, T. M., Clemens, D. P., Cohen, M., Dickey, J. M., Indebetouw, R., Jackson, J. M., Kobulnicky, H. A., Lazarian, A., Marston, A. P., Mathis, J. S., Meade, M. R., Seager, S., Stolovy, S. R., Watson, C., Whitney, B. A., Wolff, M. J., & Wolfire, M. G. 2003, PASP, 115, 953

Binney, J., & Merrifield, M. 1998, Galactic astronomy (Galactic astronomy / James Binney and Michael Merrifield. Princeton, NJ : Princeton University Press, 1998. (Princeton series in astrophysics) QB857 .B522 1998 ($35.00))

Boss, A. P. 1997, Science, 276, 1836

Bryden, G., Beichman, C. A., Trilling, D. E., Rieke, G. H., Holmes, E. K., Lawler, S. M., Stapelfeldt, K. R., Werner, M. W., Gautier, T. N., Blaylock, M., Gordon, K. D., Stansberry, J. A., & Su, K. Y. L. 2006, ApJ, 636, 1098

Butkevich, A. G., Berdyugin, A. V., & Teerikorpi, P. 2005, A&A, 435, 949

Calvet, N., D'Alessio, P., Hartmann, L., Wilner, D., Walsh, A., & Sitko, M. 2002, ApJ, 568, 1008

Carpenter, J. M., Mamajek, E. E., Hillenbrand, L. A., & Meyer, M. R. 2006, ApJ, 651, L49

Chen, C. H., & Jura, M. 2001, ApJ, 560, L171

Chen, C. H., Jura, M., Gordon, K. D., & Blaylock, M. 2005, ApJ, 623, 493

Chen, C. H., Sargent, B. A., Bohac, C., Kim, K. H., Leibensperger, E., Jura, M., Najita, J., Forrest, W. J., Watson, D. M., Sloan, G. C., & Keller, L. D. 2006, ApJS, 166, 351

Cieza, L., Padgett, D. L., Stapelfeldt, K. R., Augereau, J.-C., Harvey, P., Evans, II, N. J., Merín, B., Koerner, D., Sargent, A., van Dishoeck, E. F., Allen, L., Blake, G., Brooke, T., Chapman, N., Huard, T., Lai, S.-P., Mundy, L., Myers, P. C., Spiesman, W., & Wahhaj, Z. 2007, ApJ, 667, 308

Cox, A. N. 2000, Allen's astrophysical quantities (Allen's astrophysical quantities, 4th ed. Publisher: New York: AIP Press; Springer, 2000. Editedy by Arthur N. Cox. ISBN: 0387987460)

Currie, T. 2008, ArXiv e-prints, 801

Currie, T., Kenyon, S. J., Balog, Z., Rieke, G., Bragg, A., & Bromley, B. 2008, ApJ, 672, 558

Cutri, R. M., Skrutskie, M. F., van Dyk, S., Beichman, C. A., Carpenter, J. M., Chester, T., Cambresy, L., Evans, T., Fowler, J., Gizis, J., Howard, E., Huchra, J., Jarrett, T., Kopan, E. L., Kirkpatrick, J. D., Light, R. M., Marsh, K. A., McCallon, H., Schneider, S., Stiening, R., Sykes, M., Weinberg, M., Wheaton, W. A., Wheelock, S., & Zacarias, N. 2003, 2MASS All Sky Catalog of point sources.

(The IRSA 2MASS All-Sky Point Source Catalog, NASA/IPAC Infrared Science Archive. http://irsa.ipac.caltech.edu/applications/Gator/)

Dahm, S. E., & Hillenbrand, L. A. 2007, AJ, 133, 2072

de Jager, C., & Nieuwenhuijzen, H. 1987, A&A, 177, 217

Decin, G., Dominik, C., Waters, L. B. F. M., & Waelkens, C. 2003, ApJ, 598, 636

Gilmore, G., King, I. R., van der Kruit, P. C., & Buser, R. 1990, Science, 250, 703

Goldreich, P., & Ward, W. R. 1973, ApJ, 183, 1051

Gutermuth, R. A., Myers, P. C., Megeath, S. T., Allen, L. E., Pipher, J. L., Muzerolle, J., Porras, A., Winston, E., & Fazio, G. 2008, ApJ, 674, 336

Habing, H. J., Dominik, C., Jourdain de Muizon, M., Laureijs, R. J., Kessler, M. F., Leech, K., Metcalfe, L., Salama, A., Siebenmorgen, R., Trams, N., & Bouchet, P. 2001, A&A, 365, 545

Haisch, Jr., K. E., Lada, E. A., & Lada, C. J. 2001, ApJ, 553, L153

Hartmann, L., Megeath, S. T., Allen, L., Luhman, K., Calvet, N., D'Alessio, P., Franco-Hernandez, R., & Fazio, G. 2005, ApJ, 629, 881

Haywood, M., Robin, A. C., & Creze, M. 1997, A&A, 320, 440

Hernández, J., Briceño, C., Calvet, N., Hartmann, L., Muzerolle, J., & Quintero, A. 2006, ApJ, 652, 472

Hernández, J., Calvet, N., Hartmann, L., Briceño, C., Sicilia-Aguilar, A., & Berlind, P. 2005, AJ, 129, 856

Hernandez, J., Hartmann, L., Calvet, N., Jeffries, R. D., Gutermuth, R., Muzerolle, J., & Stauffer, J. 2008, ArXiv e-prints, 806

Hernandez, J., Hartmann, L., Megeath, T., Gutermuth, R., Muzerolle, J., Calvet, N., Vivas, A. K., Briceno, C., Allen, L., Stauffer, J., Young, E., & Fazio, G. 2007, ArXiv Astrophysics e-prints

Hillenbrand, L. A., Carpenter, J. M., Kim, J. S., Meyer, M. R., Backman, D. E., Moro-Martín, A., Hollenbach, D. J., Hines, D. C., Pascucci, I., & Bouwman, J. 2008, ApJ, 677, 630

Hillenbrand, L. A., Strom, S. E., Vrba, F. J., & Keene, J. 1992, ApJ, 397, 613

Høg, E., Fabricius, C., Makarov, V. V., Urban, S., Corbin, T., Wycoff, G., Bastian, U., Schwekendiek, P., & Wicenec, A. 2000, A&A, 355, L27

Johnson, H. L. 1966, ARA&A, 4, 193

Kharchenko, N. V. 2001, Kinematika i Fizika Nebesnykh Tel, 17, 409

Kobulnicky, H. A., Monson, A. J., Buckalew, B. A., Darnel, J. M., Uzpen, B., Meade, M. R., Babler, B. L., Indebetouw, R., Whitney, B. A., Watson, C., Churchwell, E., Wolfire, M. G., Wolff, M. J., Clemens, D. P., Shah, R., Bania, T. M., Benjamin, R. A., Cohen, M., Dickey, J. M., Jackson, J. M., Marston, A. P., Mathis, J. S., Mercer, E. P., Stauffer, J. R., Stolovy, S. R., Norris, J. P., Kutyrev, A., Canterna, R., & Pierce, M. J. 2005, AJ, 129, 239

Kuiper, G. P. 1951, Proceedings of the National Academy of Science, 37, 1

Kurucz, R. 1993, ATLAS9 Stellar Atmosphere Programs and 2 km/s grid. Kurucz CD-ROM No. 13. Cambridge, Mass.: Smithsonian Astrophysical Observatory, 1993., 13

Lada, C. J., Muench, A. A., Luhman, K. L., Allen, L., Hartmann, L., Megeath, T., Myers, P., Fazio, G., Wood, K., Muzerolle, J., Rieke, G., Siegler, N., & Young, E. 2006, AJ, 131, 1574

Lagrange, A.-M., Backman, D. E., & Artymowicz, P. 2000, Protostars and Planets IV, 639

Malmquist, K. G. 1922, journMedd. Lund. Obs., 32

Mamajek, E. E., Meyer, M. R., Hinz, P. M., Hoffmann, W. F., Cohen, M., & Hora, J. L. 2004, ApJ, 612, 496

Mannings, V., & Barlow, M. J. 1998, ApJ, 497, 330

Megeath, S. T., Hartmann, L., Luhman, K. L., & Fazio, G. G. 2005, ApJ, 634, L113

Mercer, E. P., Clemens, D. P., Meade, M. R., Babler, B. L., Indebetouw, R., Whitney, B. A., Watson, C., Wolfire, M. G., Wolff, M. J., Bania, T. M., Benjamin, R. A., Cohen, M., Dickey, J. M., Jackson, J. M., Kobulnicky, H. A., Mathis, J. S., Stauffer, J. R., Stolovy, S. R., Uzpen, B., & Churchwell, E. B. 2005, ApJ, 635, 560

Metchev, S. A., Hillenbrand, L. A., & Meyer, M. R. 2004, ApJ, 600, 435

Meyer, M. R., Backman, D. E., Weinberger, A. J., & Wyatt, M. C. 2006, ArXiv Astrophysics e-prints

Mizuno, H. 1980, Progress of Theoretical Physics, 64, 544

Moór, A., Ábrahám, P., Derekas, A., Kiss, C., Kiss, L. L., Apai, D., Grady, C., & Henning, T. 2006, ApJ, 644, 525

Mordasini, C., Alibert, Y., Benz, W., & Naef, D. 2007, ArXiv e-prints, 710

Moro-Martín, A., Carpenter, J. M., Meyer, M. R., Hillenbrand, L. A., Malhotra, R., Hollenbach, D., Najita, J., Henning, T., Kim, J. S., Bouwman, J., Silverstone, M. D., Hines, D. C., Wolf, S., Pascucci, I., Mamajek, E. E., & Lunine, J. 2007, ApJ, 658, 1312

Najita, J. R., Strom, S. E., & Muzerolle, J. 2007, MNRAS, 378, 369

Oudmaijer, R., Groenewegen, M. A. T., & Schrijver, H. 1999, A&A, 341, L55

Perryman, M. A. C., Lindegren, L., Kovalevsky, J., Hoeg, E., Bastian, U., Bernacca, P. L., Crézé, M., Donati, F., Grenon, M., van Leeuwen, F., van der Marel, H., Mignard, F., Murray, C. A., Le Poole, R. S., Schrijver, H., Turon, C., Arenou, F., Froeschlé, M., & Petersen, C. S. 1997, A&A, 323, L49

Plets, H., & Vynckier, C. 1999, A&A, 343, 496

Rhee, J. H., Song, I., Zuckerman, B., & McElwain, M. 2007, ApJ, 660, 1556

Rieke, G. H., Su, K. Y. L., Stansberry, J. A., Trilling, D., Bryden, G., Muzerolle, J., White, B., Gorlova, N., Young, E. T., Beichman, C. A., Stapelfeldt, K. R., & Hines, D. C. 2005, ApJ, 620, 1010

Sicilia-Aguilar, A., Hartmann, L., Calvet, N., Megeath, S. T., Muzerolle, J., Allen, L., D'Alessio, P., Merín, B., Stauffer, J., Young, E., & Lada, C. 2006, ApJ, 638, 897

Siess, L., Dufour, E., & Forestini, M. 2000, A&A, 358, 593

Skrutskie, M. F., Dutkevitch, D., Strom, S. E., Edwards, S., Strom, K. M., & Shure, M. A. 1990, AJ, 99, 1187

Spangler, C., Sargent, A. I., Silverstone, M. D., Becklin, E. E., & Zuckerman, B. 2001, ApJ, 555, 932

Strader, J., & Kobulnicky, H. A. 2008, ArXiv e-prints, 808

Strom, K. M., Strom, S. E., Edwards, S., Cabrit, S., & Skrutskie, M. F. 1989, AJ, 97, 1451

Strom, S. E., & Najita, J. 2005, in Protostars and Planets V, 8078–+

Su, K. Y. L., Rieke, G. H., Stansberry, J. A., Bryden, G., Stapelfeldt, K. R., Trilling, D. E., Muzerolle, J., Beichman, C. A., Moro-Martin, A., Hines, D. C., & Werner, M. W. 2006, ApJ, 653, 675

Uzpen, B., Kobulnicky, H. A., Monson, A. J., Pierce, M. J., Clemens, D. P., Backman, D. E., Meade, M. R., Babler, B. L., Indebetouw, R., Whitney, B. A., Watson, C., Wolfire, M. G., Benjamin, R. A., Bracker, S., Bania, T. M., Cohen, M., Cyganowski, C. J., Devine, K. E., Heitsch, F., Jackson, J. M., Mathis, J. S., Mercer, E. P., Povich, M. S., Rho, J., Robitaille, T. P., Sewilo, M., Stolovy, S. R., Watson, D. F., Wolff, M. J., & Churchwell, E. 2007, ApJ, 658, 1264

Uzpen, B., Kobulnicky, H. A., Olsen, K. A. G., Clemens, D. P., Laurance, T. L., Meade, M. R., Babler, B. L., Indebetouw, R., Whitney, B. A., Watson, C., Wolfire, M. G., Wolff, M. J., Benjamin, R. A., Bania, T. M., Cohen, M., Devine, K. E., Dickey, J. M., Heitsch, F., Jackson, J. M., Marston, A. P., Mathis, J. S., Mercer, E. P., Stauffer, J. R., Stolovy, S. R., Backman, D. E., & Churchwell, E. 2005, ApJ, 629, 512

Uzpen, B., Kobulnicky, H. A., Semler, D. R., Bensby, T., & Thom, C. 2008, ApJ, 685, 1264

Waters, L. B. F. M., & Waelkens, C. 1998, ARA&A, 36, 233

Wolk, S. J., & Walter, F. M. 1996, AJ, 111, 2066

Wood, K., Lada, C. J., Bjorkman, J. E., Kenyon, S. J., Whitney, B., & Wolff, M. J. 2002, ApJ, 567, 1183

Wright, C. O., Egan, M. P., Kraemer, K. E., & Price, S. D. 2003, AJ, 125, 359

Zuckerman, B., & Song, I. 2004, ApJ, 603, 738

This preprint was prepared with the AAS LaTeX macros v5.2.